Performance Assessment of Buried Pipelines at Fault Crossings[(*)]

Vasileios E. Melissianos,[a)] M.EERI, **Dimitrios Vamvatsikos,**[a)] M.EERI **and Charis J. Gantes**[a)]

A methodology for seismic performance assessment of onshore buried steel pipelines at fault crossings is presented. Probabilistic fault displacement hazard analysis is performed at first to determine the magnitude of the three fault displacement components in space. Then, three-dimensional structural analysis of the pipeline via a nonlinear beam-type finite element model allows accounting for the different effect of imposed displacements in each axis. Finally, convolving of seismic hazard and structural response results in joint hazard surfaces of compressive and tensile strains that can be used to estimate the mean annual rate of exceeding any limit-state of interest under the influence of demand and capacity uncertainty.

INTRODUCTION

Buried steel fuel pipelines are crucial for the energy industry. Crossing active tectonic faults is usually inevitable in seismic areas due to restrictions in the route selection procedure. Thus, the potential for imposing large ground differential displacements on the pipeline becomes the major cause of pipeline failure in fault crossing areas (O' Rourke and Liu 1999). The evaluation of pipe mechanical behavior due to seismic fault rupture has drawn the attention of numerous researchers that have conducted analytical, numerical and experimental studies (e.g. Karamitros et al. 2011, Vazouras et al. 2015 and Wijewickreme et al. 2009, respectively). However, considering that pipelines are hazardous structures, carrying out a comprehensive seismic performance assessment of buried pipeline – fault crossings becomes crucial. The assessment should incorporate the uncertainty of the loading (fault offset), the pipeline structural response (demand) and limit-state capacity (see also Wijewickreme et al. 2005). The seismic risk analysis can then become a tool to (i) design or

---

[a)] Institute of Steel Structures, School of Civil Engineering, National Technical University of Athens, 9 Iroon Polytechneiou str., Zografou Campus, GR 15780 Athens, Greece

[(*)] Based on two short papers presented in the 5th ECCOMAS 2015 Thematic Conference on Computational Methods in Structural Dynamics and Earthquake Engineering and the ASME 2015 Pressure Vessels & Piping Conference.

evaluate financial (insurance) and physical (retrofitting or upgrading) mitigating measures against the consequences of faulting, (ii) take more rational and cost-effective decisions during the route selection procedure and (iii) for developing measures to control the subsequent levels of risk through redirecting the design procedure of the earthquake-resistant design (vulnerability assessment).

In the present study such a methodology is presented. The seismic risk assessment is based on the probabilistic performance assessment framework of Cornell and Krawinkler (2000) and consists of: (i) seismic hazard analysis for quantification of the probabilistic nature of fault displacement, (ii) pipeline structural analysis for assessment of the pipe mechanical behavior and (iii) results combination for estimation of the seismic risk. In each step, the effect of uncertainties is quantified and propagated to the end result.

SEISMIC HAZARD ANALYSIS

The significant consequences of a potential pipeline failure necessitate the implementation of probabilistic approaches to evaluate any potential failure throughout the pipeline lifetime. Thus, as a first step, Probabilistic Seismic Hazard Analysis (PSHA) is used to quantify the probabilistic nature of earthquake effects and the commonly accepted incomplete knowledge regarding the complexity of the pipeline – soil interacting system.

FAULT DISPALCEMENT HAZARD

The most suitable tool to quantify the probabilistic nature of fault movement is the Probabilistic Fault Displacement Hazard Analysis (PFDHA). The basis of PFDHA has been established by Youngs et al. (2003) and further extended/applied by several researchers (Angell et al. 2003, Chen and Petersen 2011, Moss and Ross 2011, Liu et al. 2013). PFDHA aims at quantifying the mean annual rate (MAR) of exceeding arbitrary fault displacement levels at a site by considering the fault geometry, the fault slip rate, the distribution of earthquakes, as well as the corresponding epistemic and aleatory uncertainties. Herein, the "earthquake approach" of PFDHA by Youngs et al. (2003) is adopted, as derived from classic PSHA (Cornell 1968). Then, the MAR of exceeding arbitrary fault displacement values *d* at a fault crossing of interest is evaluated as:

$$\lambda_D(d) = v \int_{M_{\min}}^{M_{\max}} f_M(m) \left[\int_0^{\infty} f(r \mid m) P(D > d \mid m, r) \, \mathrm{d}r \right] \mathrm{d}m \tag{1}$$

where v is the mean annual rate (seismic rate) of all earthquakes above a minimum earthquake magnitude of engineering significance $M_{\min}$ occurring at the fault studied, $f_M(m)$ is the probability density of earthquake magnitude that the fault can produce between limiting values $M_{\min}$ and $M_{\max}$, e.g. according to the Gutenberg–Richter (1944) Bounded Recurrence Law, $f(r|m)$ is the conditional probability density function of the distance from the site of interest given an earthquake of magnitude m occurring and finally the term $P(D>d|m,r)$ is the conditional probability that, given an earthquake of magnitude m on the fault and at a distance r from the site of interest, the fault displacement D at the pipeline crossing will exceed d. The displacement prediction (attenuation) function $P(D>d|m,r)$ is the product of the conditional probability of slip, which determines whether fault displacement has appeared on the surface, and the conditional probability of displacement exceedance given that surface slip has occurred. It is noted that wherever distinction is needed, the random variables are denoted by uppercase letters (e.g. D), while their potential values by lowercase letters (e.g. d).

The "principal faulting" approach is adopted within PFDHA (Youngs et al. 2003), assuming that the pipeline intercepts a main fault, while distributed faulting issues are neglected. The "principal faulting" concept is compatible with displacement along a single narrow trace (i.e. planar fault without thickness). The fault displacement hazard estimation depends on four elements: (i) earthquake magnitude, (ii) surface rupture length, (iii) position of the surface rupture length along the fault trace, and (iv) position of the crossing site. The earthquake magnitude stands as the key factor for describing a seismic source. It ranges from a minimum value of engineering significance M_{min}, assuming an insignificant impact of lower values on hazard levels, to a maximum value M_{max}, as constrained by the finite fault size. Acknowledging that even same magnitude earthquakes may rupture fault lengths of different size, the surface rupture length (SRL) along the fault trace is introduced as the second element. The third element under consideration is the SRL position along the fault trace to determine whether a rupture of a given length will intercept the crossing of the pipeline (fourth element).

Given the fault characteristics and the crossing site position, Equation 1 can be re-written to incorporate magnitude discretization into bins and explicitly account for the aforementioned elements:

$$\lambda_D(d) = v\sum_i P(D > d \mid m_i) P_M(m_i) \quad (2)$$

where $P_M(m_i)$ is the probability of magnitude M falling within the i-th bin characterized by m_i at its center. $P(D>d|m_i)$ is the probability that the fault displacement D exceeds a defined value d at the crossing site, given an earthquake of magnitude m_i has occurred. Further discretization is typically needed for estimating of this term. Firstly, discrete values of SRLs are defined (for simplicity) as integer multiples of a minimum length that is of engineering significance by relating SRL and $M_{\min}$ via the expressions of Wells and Coppersmith (1994). Lacking better information, SRLs of the same size are considered to have equal probability of rupturing. Therefore, every SRL size is accounted for at all possible locations $Pos_{k,j}$, keeping track of the cases where the rupture crosses the pipeline and thus contributes to the fault displacement hazard. Finally, we also keep track and discretize the average or the maximum displacement of the entire fault rupture, FD. Then, the probability is expressed as:

$$P(D > d \mid m_i) = \sum_j \sum_t \sum_k P\left(D > d \mid SRL_j, FD_t, Pos_{k,j}\right) P\left(SRL_j, FD_t \mid m_i\right) P\left(Pos_{k,j}\right) \quad (3)$$

The first term within the triple sum is the conditional probability of exceeding d, where detailed calculations are carried out over each combination of SRL, position of SRL relative to the crossing site, and value of FD. Given these parameters, this term becomes magnitude-independent. The second term is the joint probability of SRL and FD, conditional on the magnitude, e.g. as provided by Wells and Coppersmith (1994). The third term, $P(Pos_{k,j})$, estimates the probability of different SRL_j positions along the fault. Different positions of equal-length SRL_j values are assumed to be equiprobable and independent of the magnitude and thus the probability function is substituted by $1/N_j$, where N_j is the number of potential SRL_j positions considered. This conceptual algorithm applies for both alternative approaches of PFDHA for estimating FD. The first is based on empirical expressions for predicting the average displacement (AD) along the fault under a given event, while the second approach uses estimates for the maximum displacement (MD) appearing anywhere along the fault line. In the following, both shall be employed to offer alternative options for PFDHA.

FAULT DISPLACEMENT COMPONENTS

The focus is on a straight pipeline segment without any bends, which crosses a fault that is assumed to be planar without thickness; it appears on the ground as a straight line and thus the pipeline – fault intersection is idealized as a point. While there may be significant uncertainty regarding the actual position where the rupture will appear on the surface, its effect will disappear if we assume that the pipeline – soil system properties are invariable throughout the entire straight crossing segment considered. When that is not the case, such uncertainty should be incorporated explicitly. The pipeline – fault crossing geometry is schematically presented in Figure 1, where the fault dip angle is denoted by ψ and the pipeline – fault crossing angle by β. The fault displacement D can be represented in three dimensions by three components: Δ_1 and Δ_2 are the fault-trace-parallel and fault-trace-normal horizontal components, while Δ_3 represents the vertical component:

$$D = \sqrt{\Delta_1^2 + \Delta_2^2 + \Delta_3^2} \tag{4}$$

$$\Delta_2 = \begin{cases} \Delta_3 / \tan\psi & 0^o < \psi < 90^o \\ 0 & \psi = 90^o \end{cases} \tag{5}$$

It is noted that the fault dip angle ψ ranges from 0^o (theoretical value) to 90^o (vertical fault plane). When $\psi = 90^o$ the Δ_2 fault-trace-normal component becomes zero, as mandated by the fault geometry.

The fault (global) coordinate system (1,2,3) is rotated by the pipeline – fault crossing angle β in the horizontal plane to determine the local coordinates system (x,y,z) of the pipeline: Δ_x is the longitudinal and Δ_y is the transverse horizontal displacement with respect to the pipeline axis, while Δ_z is the pipeline vertical displacement:

$$\begin{aligned} \Delta_x &= \Delta_1 \cos\beta + \Delta_2 \sin\beta \\ \Delta_y &= -\Delta_1 \sin\beta + \Delta_2 \cos\beta \\ \Delta_z &= \Delta_3 \end{aligned} \tag{6}$$

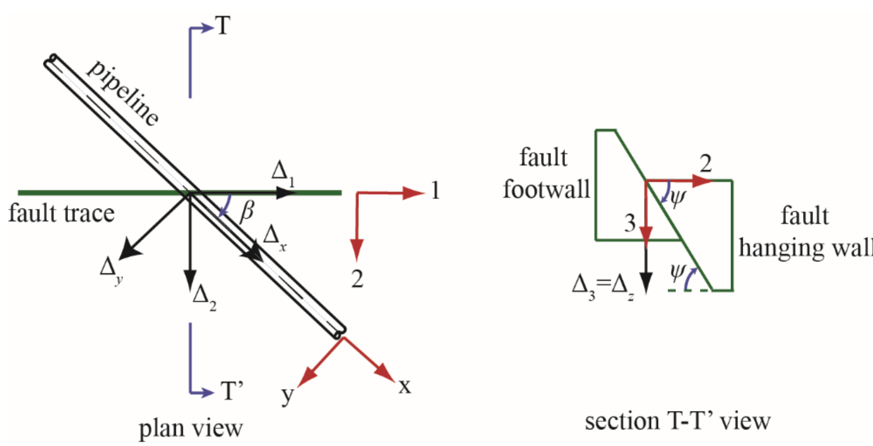

Figure 1. Pipeline – fault crossing plan and section view

Standard PFDHA deals with the fault displacement magnitude and neglects its distribution into x/y/z spatial components. The fault movement is however three-dimensional in nature, while its type (normal, strike-slip, reverse) is generally defined by the principal fault component. In cases where the principal component is the vertical Δ_3, then the fault is either normal or reverse, while if it is the horizontal Δ_1, the fault is classified as strike-slip. Thereby, the distribution of fault displacement components in 3D space corresponds to the fault type. Also, the pipeline structural response to faulting is directly related to the fault type; in addition to ubiquitous pipe bending, normal faulting induces tension, reverse faulting introduces compression, while strike-slip faults can cause either of the two, depending on the geometry. As data on the fault component distribution is usually lacking, a simple and approximate procedure is adopted where the principal component is uncertain, assuming a uniform or normal distribution within 75% to 90% of D (Table 1). Such distributions are reasonable assumptions, to be re-evaluated if adequate data become available. The lower bound of $0.75D$ stands for a rational assumption to ensure that the magnitude of the principal component is compatible with the fault type and no other component will exceed the principal one. The upper bound of $0.90D$ is based on the assumption that, while a fault is characterized by the principal component, this in nature does not exclude movement in the other two directions.

Table 1. Uniform and normal distribution parameters considered for the distribution of the principal fault displacement component (CoV = coefficient of variation)

Distribution	Parameters			
	Mean	CoV	Lower bound	Upper bound
Truncated normal	$0.80D$	0.20	$0.75D$	$0.90D$
Uniform	-	-	$0.75D$	$0.90D$

Thus, of the two independent components, Δ_1 and Δ_3, the principal one for the given faulting type is sampled according to Table 1. The other component is determined according to Equations 4 and 5 given the fault displacement magnitude D. Then, a certain bookkeeping exercise is needed of appropriately discretizing $\lambda_D(d)$, estimated by Equation 2, and distributing its constituents to bins of Δ_1 and Δ_3. This is facilitated by changing from the bins of MAR of exceedance λ_D to the bins of MAR of equaling, $\Delta\lambda_D(d)$:

$$\Delta\lambda_D\left(d\right)=\left|\lambda_D\left(d+a\right)-\lambda_D\left(d-a\right)\right|=\lambda_D\left(d-a\right)-\lambda_D\left(d+a\right) \quad (7)$$

where $2a$ is the displacement bin width. Note that whereas the differential MAR $d\lambda_D(d)$ is negative due to decreasing hazard with d, $\Delta\lambda_D(d)$ is defined to be always positive. The method becomes clearer if for example an oblique strike-slip fault ($\psi \neq 90^{o}$) is considered, where the principal component is Δ_1. The MAR of equaling is then evaluated as:

$$\Delta\lambda_{\Delta_1,\Delta_3}\left(\delta_1,\delta_3\right)=\Delta\lambda_D\left(d\right)P\left(\Delta_1\left(d\right)\in\left[\delta_1-\alpha,\delta_1+\alpha\right]\mid d\right)$$
$$\text{where} \quad d=\sqrt{\delta_1^2+\delta_3^2\left(1+\frac{1}{\tan^2\psi}\right)} \tag{8}$$

where the range of the fault displacement D and the two independent components (Δ_1, Δ_3) have been discretized into a sufficiently large number of bins. The first term, $\Delta\lambda_D$, is here estimated as the difference of the λ_D at the bin edges as per Equation 7. The second term is the probability of Δ_1 falling in a given bin characterized by central values of δ_1 and δ_3 (while both being compatible with the given fault displacement d), evaluated according to the distributions of Table 1.

HAZARD UNCERTAINTY

Any quantifiable uncertainty can be incorporated in PFDHA from its origins. Identification and quantification of uncertainties (aleatory and epistemic) is integral to seismic hazard analysis, as a hazard curve without considering the pertinent uncertainties is highly sensitive to the "certain" parameters adopted. Aleatory uncertainties are related to the inherent variability of nature, e.g. randomness in earthquake magnitude, fault location or fault displacement, and cannot be easily reduced. Seismological data with aleatory uncertainty are therefore processed through sampling. Epistemic uncertainties are related to the inadequate understanding of the nature and in time can be reduced with better observations, e.g. earthquake and ground motion models. Epistemic uncertainties lead to alternative hazard curves and are usually handled through logic trees, considered to be the state-of-the-art tool for quantifying and incorporating epistemic uncertainties in the seismic hazard calculation (Bommer and Scherbaum 2008). The development of a logic tree includes the production of alternative models for various input parameters and the assignment of weight factors to the different tree branches. Weight factors can be generally interpreted to represent the relative belief of the engineer in alternative models, without necessarily being frequency-based probabilities (Abrahamson and Bommer 2005).

An example of a potential logic tree is illustrated in Figure 2, where the seismic rate v, the maximum earthquake magnitude $M_{\max}$ and the fault displacement approach of PFDHA are considered to be uncertain. The seismic rate v is the determining feature of a seismic source, while its mean value is usually provided. Unlike the minimum magnitude M_{min} that is an engineering choice, the maximum magnitude M_{max} is an important characteristic provided by seismologists for the source under investigation. The choice of displacement approach of PFDHA, either the average displacement (AD), or the maximum displacement (MD), is also incorporated in the uncertainty analysis, due to the lack of sufficient data to accurately evaluate the alternative approaches. Finally, the principal fault displacement component distribution is also an option to consider for the estimation of 3D spatial components.

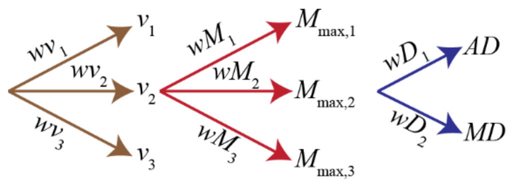

Figure 2. Potential hazard uncertainty logic tree for determining the fault displacement D hazard by considering the seismic rate v, the maximum earthquake magnitude M_{max} and the AD or MD alternative approaches of PFDHA

PIPELINE STRUCTURAL ANALYSIS

In seismic risk analysis the roles of the seismologist and the structural engineer are linked via an interface variable, known as the intensity measure (IM); for example, in building assessment a typical scalar IM is the first-mode spectral acceleration $S_a(T_1)$. For the pipeline – fault crossing assessment an appropriate scalar IM could be the fault displacement D. However, the distribution of fault displacement components in the three-dimensional space dominates the pipeline mechanical behavior. Therefore, the independent fault displacement components (Δ_1,Δ_3) are selected as a vector IM (Bazzuro and Cornell 2002). Assuming that the fault is planar at the crossing site, components Δ_1 and Δ_3 are fault displacement components that fully describe the structural model loading conditions. In cases that the proposed methodology is to be extended to encompass duration-dependent-failure, such as low-cycle fatigue, this IM may become insufficient, i.e., incapable of fully characterizing the seismic effects on the pipeline without recourse to other earthquake characteristics, and thus require improvement.

Buried pipeline design against non-seismic loads is usually based on a comparison of the pipeline stress demand to a limiting stress, according to pertinent structural codes (e.g., ASME B31.8 2012). However, in cases of earthquake-induced actions, the developing stresses are larger compared to typical working stress limits. Thus, buried pipeline design against faulting is carried out in strain terms (Strain Based Design), rather than stress terms, given that the problem is displacement-controlled. Hence, pipeline structural analysis provides strain demand (ε_{dem}) in terms of the maximum developing tensile and compressive strains. Demand is then compared against strain capacity (ε_{cap}) to assess the potential of failure.

In case of faulting and regarding the ultimate limit state that is associated to severe damage, leakage or explosion, main failure modes of a corrosion-free continuous pipeline are local buckling and tensile rupture. Compression leads to the formation of a wrinkle that may evolve to a local buckle, causing pipe local instability. Concentration of tensile strains may lead to tensile rupture of the girth welds between the adjacent pipe parts. Welds are the weakest locations and are prone to strain concentration due to the thermally affected area of the welding process. Thus, two states are defined within the ultimate limit state: (i) local buckling due to compressive strains (LS_c) and (ii) tensile rupture due to tensile strains (LS_t).

PIPELINE STRAIN HAZARD ANALYSIS

The assessment approach is based on a simplified version of the Cornell – Krawinkler framing equation adopted by the Pacific Earthquake Engineering Research (PEER) Center (Cornell and Krawinkler 2000):

$$\lambda_{LS} = \int G\left(EDP \mid IM\right)\left|\mathrm{d}\lambda\left(IM\right)\right| \tag{9}$$

For pipeline – fault crossings, the engineering demand parameters (EDP) are the tensile and compressive strains, the intensity measure (IM) is the vector of the fault components Δ_1 and Δ_3 and $G(EDP|IM)$ represents the probability of exceeding values of the EDP given the vector IM, defining a fragility surface. Thus, Equation 9 becomes a double integral over the two IM components:

$$\lambda_{LS} = \lambda_{\varepsilon_{dem} > \varepsilon_{cap}} = \int_0^{+\infty}\int_0^{+\infty} P\left(\varepsilon_{dem} > \varepsilon_{cap} \mid \delta_1, \delta_3\right)\mathrm{d}\lambda_{\Delta_1,\Delta_3}\left(\delta_1, \delta_3\right) \tag{10}$$

where $\mathrm{d}\lambda_{\Delta_1,\Delta_3}\left(\delta_1, \delta_3\right)$ is the MAR differential of fault displacement components obtained from Equation 8 and $P(\varepsilon_{dem}>\varepsilon_{cap}|\delta_1,\delta_3)$ is the probability of strain demand exceeding strain capacity estimated for given/specified values δ_1, δ_3 of the fault components, i.e. the fragility function. By appropriate discretization, the integrals of Equation 10 are substituted by easier-to-compute summations:

$$\lambda_{LS} = \sum_i \sum_j P\left(\varepsilon_{dem} > \varepsilon_{cap} \mid \delta_{1,i}, \delta_{3,j}\right) \Delta\lambda_{\Delta_1,\Delta_3}\left(\delta_{1,i}, \delta_{3,j}\right) \tag{11}$$

Limit state assessment can incorporate the uncertainty of both strain demand and strain capacity. The simpler case of course is to treat both as non-random variables by neglecting the uncertainty, e.g. with respect to the structural model parameters (demand) and the limit-state threshold values (capacity). It is noteworthy that for buried pipelines at fault crossing there is no appreciable "record-to-record" variability in practice (i.e. dispersion of EDP given IM), compared to the usual procedure in building assessment (e.g. Vamvatsikos and Cornell 2002). In other words, given the intensity measure values Δ_1 and Δ_3, there is little uncertainty in the level of pipeline demand that is not model-related in contrast to building assessment studies where the ground motion records can impart significant variability for a given value of $S_a(T_1)$. Thus, variability in demand given the fault displacement components is derived mainly from the model uncertainty (e.g. in soil properties) that is not easy to quantify and therefore it may not be unusual to assume that strain demand is practically deterministic given fault displacement components Δ_1 and Δ_3.

Code-based strain limits are adopted for defining strain capacity. Tensile and compressive strain limits suggested by ALA (2001) are listed in Table 2, where t is the pipe wall thickness, D_e is the external diameter, $D_{\min}$ is the minimum inside diameter, E is the steel modulus of elasticity and p the internal pressure. Code-based strain limits usually result from conservative fitting of experimental results, while additional safety factors are also incorporated in the final expressions. Unbiased mean or median values, which may be considerably larger, are thus preferable for proper assessment.

Table 2. Deterministic strain capacity suggested by ALA (2001)

Limit state	Tensile strain	Compressive strain
Operable	2%	$0.5\left(t/D'\right) - 0.0025 + 3000\left(pD_e/2Et\right)^2$, $D' = D_e/\left[1 - 3\left(D_e - D_{\min}\right)/D_e\right]$
Pressure integrity	4%	$1.76t/D_e$

Using Equation 11, strain hazard curves (or surfaces) can also be constructed. Strain hazard curves are a useful visual tool for understanding the performance of the pipeline, showing the MAR of exceeding arbitrary values of strain demand. They can also be employed for simplified assessment limit-state exceedance assuming that the corresponding strain capacity is deterministic. The first step is to estimate strain demand for every combination of fault displacement components. A useful strategy for computational efficiency is to perform pipeline structural analysis for parameters that convey the entire range of pipeline response, from no damage to leakage or rupture, akin to an Incremental Dynamic Analysis (Vamvatsikos and Cornell 2002). Secondly, the strain hazard curves are constructed by convolving the hazard and structural analysis results through the IM. To do so, a range of tensile (ε_t) and compressive strains (ε_c) is selected by the engineer to cover the anticipated range of the response values. This 2D space of strain values is then discretized into a number of (ε_t, ε_c) bins and the strain hazard is calculated at each bin by summing the MAR of equaling values corresponding to tensile and compressive strains that cause exceedance (violation) of the limit-state.

All such strain hazard or limit-state MAR assessments depend on the accurate estimation of the probability of exceedance term in Equation 11, a calculation that depends on whether uncertainty is incorporated in demand and capacity. In the special case where the strain demand and capacity are assumed to be non-random, the fragility function of Equation 11 becomes a step function:

$$P\left(\varepsilon_{dem} > \varepsilon_{cap} \mid \delta_{1,i}, \delta_{3,j}\right) = \begin{cases} 0, & \varepsilon_{dem} < \varepsilon_{cap} \\ 1, & \varepsilon_{dem} > \varepsilon_{cap} \end{cases} \tag{12}$$

The MAR of equaling $\Delta\lambda_\varepsilon(\varepsilon_c,\varepsilon_t)$ for strains that fall within each bin is estimated via the expression:

$$\Delta\lambda_\varepsilon\left(\varepsilon_c, \varepsilon_t\right) = \sum_i \sum_j P\left(\varepsilon_{c,ij} \in I\left[\varepsilon_c\right] \text{ and } \varepsilon_{t,ij} \in I\left[\varepsilon_t\right]\right) \Delta\lambda_{\Delta_1,\Delta_3}\left(\delta_{1,i}, \delta_{3,j}\right) \tag{13}$$

where $\varepsilon_{c,\mathrm{ij}}$ and $\varepsilon_{t,\mathrm{ij}}$ are the compressive and tensile strain estimates for concurrent displacement components $\delta_{1,i}$ and $\delta_{3,j}$. $I[\varepsilon_c]$ denotes the interval $[\varepsilon_c - a, \varepsilon_c + a]$, where a is the bin width for discretizing compressive strains and $I[\varepsilon_t] \equiv [\varepsilon_t - b, \varepsilon_t + b]$, where b is the bin width for discretizing tensile strains. For non-random demand and capacity, the MAR of equaling $\Delta\lambda_\varepsilon(\varepsilon_c,\varepsilon_t)$ given ε_c and ε_t is practically estimated by summing the MAR of equaling values for strains that fall within the failure region (i.e. they exceed the respective capacity).

Considering then the demand as deterministic and the capacity as uncertain, the fragility function of Equation 11 yields:

$$P\left(\varepsilon_{dem} > \varepsilon_{cap} \mid \delta_{1,i}, \delta_{3,j}\right) = \sum_{n=1}^{N}\left(\begin{cases}0, & \varepsilon_{dem} < \varepsilon_{cap,n} \\ 1, & \varepsilon_{dem} > \varepsilon_{cap,n}\end{cases}\right)\frac{1}{N} \tag{14}$$

where the capacity distribution is discretized into N equiprobable points $\varepsilon_{cap,n}$ using for example stratified or random sampling.

Finally, considering the general case for both demand and capacity being uncertain parameters, the fragility function of Equation 11 yields:

$$P\left(\varepsilon_{dem} > \varepsilon_{cap} \mid \delta_{1,i}, \delta_{3,j}\right) = \int_{0}^{+\infty} P\left(\varepsilon_{dem}\left(\delta_{1,i}, \delta_{3,j}\right) > \varepsilon_{cap} \mid \delta_{1,i}, \delta_{3,j}, \varepsilon_{cap}\right) P\left(\varepsilon_{cap}\right) \mathrm{d}\varepsilon_{cap} \tag{15}$$

Using then a sufficiently fine discretization, the integral of Equation 15 can be replaced by summations, over N equiprobable $\varepsilon_{cap,n}$ values:

$$P\left(\varepsilon_{dem} > \varepsilon_{cap} \mid \delta_{1,i}, \delta_{3,j}\right) = \sum_{n=1}^{N} P\left(\varepsilon_{dem}\left(\delta_{1,i}, \delta_{3,j}\right) > \varepsilon_{cap,n} \mid \delta_{1,i}, \delta_{3,j}, \varepsilon_{cap,n}\right) / N \tag{16}$$

The probability of the right-hand term of Equation 16 is essentially the cumulative distribution function of ε_{dem} evaluated at given values of sampled capacity $\varepsilon_{cap,n}$. For example, assuming that demand follows a lognormal distribution, the exceedance probability term can be expressed as:

$$P\left(\varepsilon_{dem}\left(\delta_{1,i}, \delta_{3,j}\right) > \varepsilon_{cap,n} \mid \delta_{1,i}, \delta_{3,j}, \varepsilon_{cap,n}\right) = \Phi\left(\frac{\ln \varepsilon_{dem}\left(\delta_{1,i}, \delta_{3,j}\right) - \ln \varepsilon_{cap,n}}{\sigma_{\ln \varepsilon_{dem}}}\right) \tag{17}$$

CASE STUDY

As a case study, a typical high-pressure natural gas API5L-X65 pipeline is considered, featuring an external diameter of 914mm (36in) and a wall thickness of 12.7mm. The internal pressure of the pipe is not considered as a less favorable situation. The steel is considered to be elastoplastic with isotropic hardening. The pipeline is coated with coal tar and buried under 1.30m of medium-density cohesionless sand with internal friction angle 36^{o} and unit weight $18kN/m^3$. A pipeline – normal fault crossing is then considered with fault length equal to 40km, pipe crossing located 10km from the fault closest edge and angles $\psi = 70^{o}$ and $\beta = 80^{o}$ (see Figure 1). The adopted seismological parameters of the fault (seismic rate v, minimum and maximum earthquake magnitude) and the corresponding uncertainty weight factors are listed in Table 3, together with the weighting of the AD and MD approach of PFDHA. It is noted that the selected seismic rates are indicative of highly active faults.

Table 3. Case study seismological parameters and uncertainty weight factors, M_{min} = 4.50

Parameter	Weight factor	Parameter	Weight factor	Parameter	Weight factor
$v_1 = 1.60$	$wv_1 = 0.30$	$M_{max,1} = 7.00$	$wM_1 = 0.25$	AD	$wD_1 = 0.50$
$v_2 = 2.00$	$wv_2 = 0.40$	$M_{max,2} = 7.20$	$wM_2 = 0.45$	MD	$wD_2 = 0.50$
$v_3 = 2.40$	$wv_3 = 0.30$	$M_{max,3} = 7.40$	$wM_3 = 0.30$		

SEISMIC HAZARD ANALYSIS

The mean fault displacement hazard curve at the pipeline crossing site is illustrated in Figure 3(a). The rapidly descending curve shape is predictable as the lower the fault displacement is, the higher becomes the MAR of exceeding. The mean hazard curve is shown in Figure 3(b) together with the plus/minus one standard deviation curves. The significant dispersion that is identified in Figure 3(b) depends on the selected seismological parameters and mainly the seismic rate v considered. The MAR of equaling for the independent fault displacement components Δ_1 and Δ_3 is presented in Figure 4. This surface can be used to evaluate the rate of components reaching a specific value with reference to the fault type and the fault displacement magnitude.

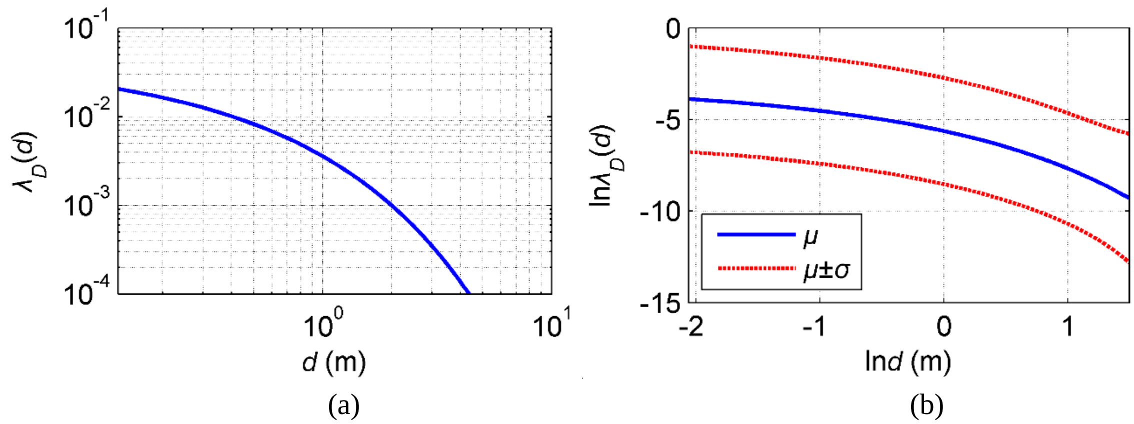

Figure 3. (a) Mean fault displacement hazard curve on pipeline crossing site, (b) Mean fault displacement hazard curve and its dispersion due to uncertainty

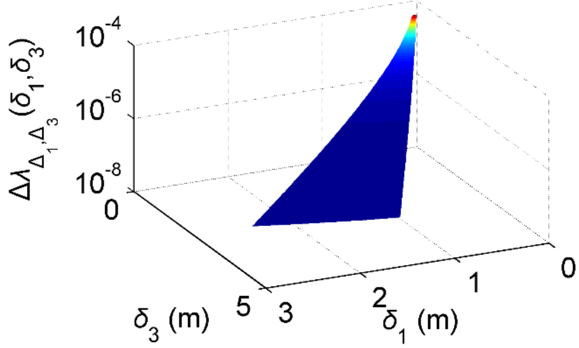

Figure 4. MAR of equaling surface for the independent fault displacement components Δ_1, Δ_3, where lower MAR values are associated with increasingly larger displacement components in both directions, thus showing this characteristic widening of the surface

The conditional probability of exceeding fault displacement values is the core of PFDHA and within it the normalization of fault displacement values can be carried out using either the average displacement (AD) or the maximum fault displacement (MD) approach. The identification of the AD versus MD approach impact on λ_D calculation cannot be discounted. Figure 5 illustrates that, at least for the case at hand, both approaches yield nearly identical result for low displacements, but then the AD approach leads to higher rates for any value of displacement larger than about 1m, while also maintaining a lower hazard slope throughout. Given the equal weighting adopted (Table 3), the final mean hazard curve is essentially the average of the two.

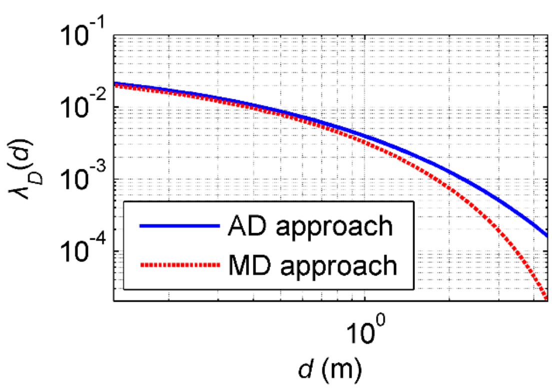

Figure 5. Mean fault displacement hazard curve adopting the AD versus the MD approach

PIPELINE STRUCTURAL ANALYSIS

A beam-type finite element model is developed to assess the pipe mechanical behavior due to faulting, as suggested by pertinent structural codes (e.g. ALA 2001). The total modeled length is 1000m and the fault is assumed to intercept the pipeline at the middle-span of the modeled length. Geometrically and materially nonlinear numerical analysis is performed using the general purpose FEM software ADINA (2008). The pipeline is meshed with beam-type elements of 0.25m length, while the surrounding soil is modeled with nonlinear spring elements whose properties are estimated according to ALA (2001) provisions.

The engineering demand parameters of interest are the maximum tensile and compressive strain demand appearing anywhere along the modeled length. Failure modes such as local buckling and tensile rupture generally occur at different locations along the pipeline, as soil resistance, pipe – fault crossing angle, fault type and fault offset magnitude heavily affect the structural response and the case of maximum tensile and compressive strain coexistence at the same location along the pipeline is rather rare. The corresponding response surface in terms of tensile and compressive strain demands appears in Figure 6. Therein, a comprehensive view of pipeline response is shown for a wide range of the independent fault displacement components Δ_1 and Δ_3. It is, however, more efficient to perform a reduced set of structural analyses for the combination of fault displacement components that are consistent with the geometry of the pipeline – fault system for the fault crossing under investigation. Thus, in Figure 6 for the normal fault crossing considered with fault dip angle ψ = 70^o and pipe – fault crossing angle β = 80^o, only the sectors marked by crosses are physically realizable. As the pipeline is subjected to large offsets of normal faulting, tension dominates the pipe response, thus compressive strains are limited, even further constraining the range of realistic values in Figure 6b.

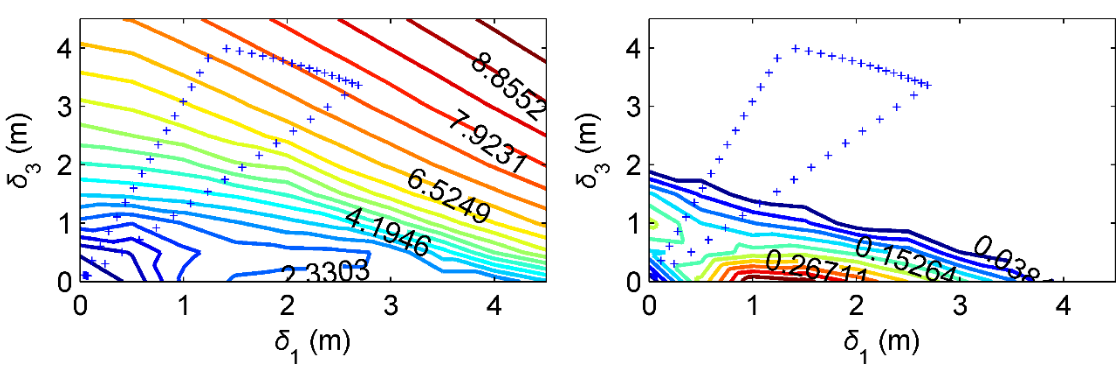

(a) (b)

Figure 6. Pipeline structural response: (a) tensile strain demand and (b) compressive strain demand

PIPELINE STRAIN HAZARD ANALYSIS

Strain hazard is the combination product of seismic hazard and structural analysis. Seismic hazard results, within the scope of the case study, are represented by their mean values accounting also for all pertinent uncertainties. The MARs of limit states can be estimated by considering strain demand and/or capacity as either deterministic or probabilistic. In the latter case, strain capacity is assumed to be normally distributed with the distribution parameters listed in Table 4. Specifically, for compressive strain, the corresponding limits (ALA 2001) are generally based on laboratory testing of pipes subjected to bending without considering the beneficial effect of the surrounding soil. The compressive limit expressions thus produced are actually conservatively estimated enveloping curves rather than true regressions capturing the central values of the data. Thus, such limits tend to be conservative, leading us to adopt an approximate 20% bias between the real mean value of the experimental results and the design code estimates. This assumed bias is based on judgement and observations of the results from Gresnigt and Karamanos (2009). On the other hand, the probabilistic strain demand is assumed to be estimated without bias from the structural model, following a lognormal distribution with 30% dispersion, mainly due to soil randomness in the vicinity of the fault.

Table 4. Strain capacity normal distribution parameters (CoV = coefficient of variation)

Parameter	Tensile strain	Compressive strain
Mean value	See Table 2	see Table 2
CoV	20%	20%
Assumed bias	-	20%

Assuming that strain demands and capacities are deterministic, the latter equal to the mean values of Table 4, the MAR of equaling strains after Equation 13 is plotted in Figure 7. Therein, the compressive strain demand remains sufficiently below the code-based limit, while tensile strain demand exceeds the corresponding limit for this tension-dominated setting only for some rare events. The decomposition of Figure 7 for tensile and compressive strains yields Figure 8(a) and Figure 8(b). The MAR of equaling strain curves are similar to marginal probability mass functions and provide the MAR of the strain reaching a defined value. The corresponding hazard curves for tensile and compressive strains are plotted in Figure 9, where the strain values appear on the horizontal axis and the MAR of exceeding the strain demand on the vertical axis. The effect of demand and capacity uncertainties are evaluated in Table 5, where the estimated limit MAR is listed. In general, ignoring dispersion in either can lead to erroneous results. In the examined case, demand and capacity uncertainties have minor effect on the limit MAR, as a well-constructed pipe without significant uncertainties is considered, thus dominated by the hazard uncertainty. In the opposite case, if an aging pipeline was considered with uncertain material/condition pipe, then demand and capacity uncertainties might become quite more important.

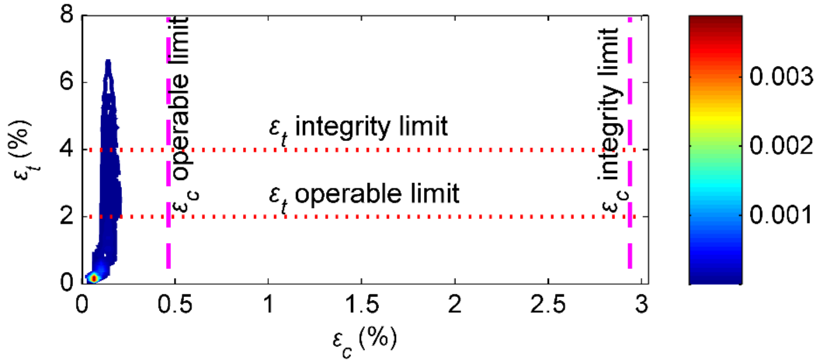

Figure 7. Contours of the MAR of equaling for combinations of tensile and compressive strain demands against the corresponding mean capacity values (deterministic demand and capacity assumed)

To better understand the results shown, the pipeline fragility surface for tensile fracture are depicted in Figure 10, where the probability of strain demand exceeding strain capacity (Equation 16) is plotted versus the selected vector intensity measure (i.e. the independent fault displacement components Δ_1 and Δ_3). On the other hand, the local buckling probability has been shown to be very low and the corresponding fragility curves cannot provide useful information. The reason is that the pipe response in the examined case is mainly tensional due to the following facts: (i) the considered fault dip angle is $\psi = 70^o$ (a relatively common value in nature for normal faults) leading to increased pipe tension rather than bending, in contrast, e.g., to the case of $\psi = 90^o$, where the pipe would be mainly subjected to bending; (ii) the considered pipeline – fault crossing angle is $\beta = 80^o$ and thus pipeline is subjected to tension apart from bending and (iii) although the fault is normal, movement along the fault plane, i.e. the fault-parallel horizontal component of Figure 1, is not zero, thus increasing the tensional load.

Table 5. MAR of exceeding limit state in tension ($\lambda_{LS,t}$) and compression ($\lambda_{LS,c}$)

		Operable conditions		Pressure integrity	
Demand	Capacity	$\lambda_{LS,t}$	$\lambda_{LS,c}$	$\lambda_{LS,t}$	$\lambda_{LS,c}$
non-random	non-random	0.0025	0	0.00076	0
non-random	random	0.0026	0	0.00084	0

random	random	0.0027	2.83×10^{-7}	0.00930	1.69×10^{-18}

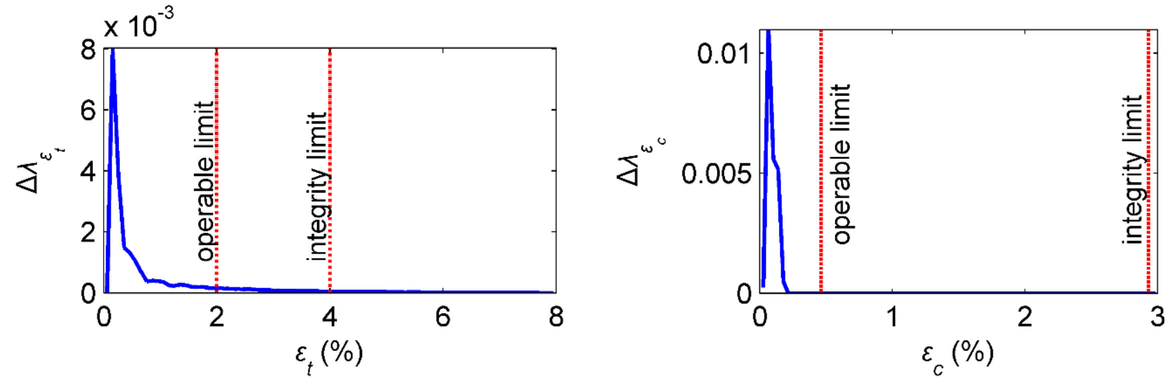

Figure 8. Tensile (ε_t) and compressive (ε_c) strains MAR of equaling (deterministic demand and capacity)

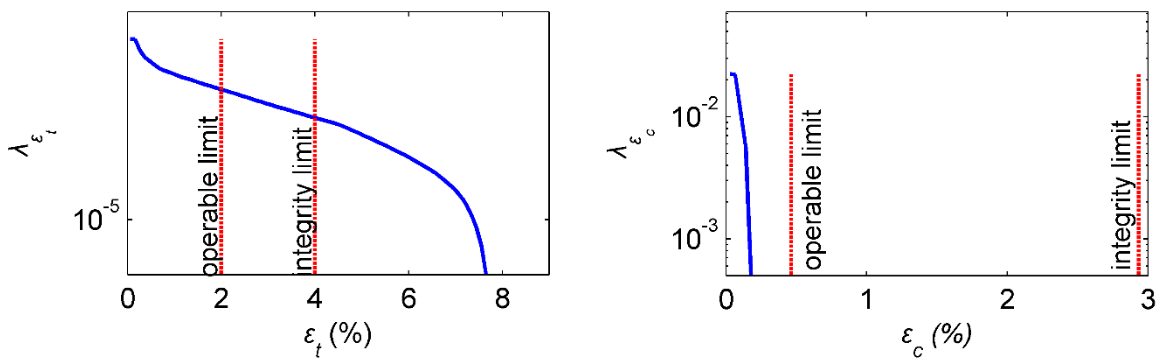

Figure 9. Tensile (ε_t) and compressive (ε_c) strains hazard curves (deterministic demand and capacity)

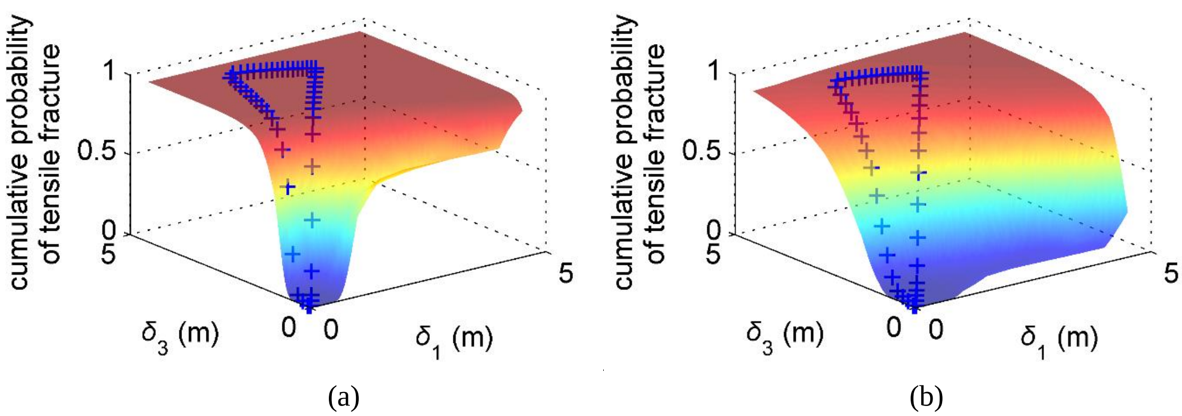

Figure 10. Cumulative probability of tensile fracture (random demand and capacity) using (a) the operable or (b) the pressure integrity tensile limit as the mean value of capacity, where the crosses indicate the range of physically possible combinations for the given pipeline – fault geometry

DETERMINISTIC VERSUS PROBABILISTIC APPROACH

Pipeline design against tectonic fault rupture is usually carried out in a deterministic way. It is thus essential to demonstrate the differences between the deterministic and the probabilistic analysis approach. In order to obtain qualitative and quantitative understanding of the way that each method handles the pipe assessment, the three step procedure followed in the probabilistic approach will be adopted also in the deterministic one, albeit for a single “design” scenario. Therefore, the first step is the estimation of the seismic load, i.e. the fault offset magnitude. Empirical expressions using geometrical characteristics of the fault are usually employed. Herein, the fault rupture length equals 40km and the fault offset for normal faulting is estimated after Wells and Coppersmith (1994):

$$\log\left(\hat{D}_{\text{average}}\right) = -1.99 + 1.24\log\left(SRL\right) \tag{18}$$

where $\hat{D}_{\text{average}}$ is the median estimate of the average fault displacement. Here, the AD rather than the MD approach is employed, based on the suggestions of Wells and Coppersmith (1994) as the maximum fault displacement is improbable to occur at the pipe crossing. *SRL* is assumed to be equal to the entire fault length as only a single scenario of fault rupture is considered. Therefore, Equation 18 yields a median (50%) estimate of $\hat{D}_{\text{average}}$ = 0.99m. For additional safety, the 84% estimate of 2.33m may be used. Proceeding to the second step, namely the pipe structural analysis, the principal fault displacement component Δ_3 is assumed to equal the corresponding upper bound of Table 1 with respect to fault offset magnitude, while the other two components are estimated via Equations (4) and (5). Thus, the obtained fault displacement components are Δ_1 = 1.51m, Δ_2 = 0.76m and Δ_3 = 2.09m. The maximum longitudinal tensile strain obtained from structural analysis is 3.39% and the compressive one is 0.13%. Without introducing any additional safety factors to add conservatism and using the strain limits of Table 2, it is concluded that the pipe will not fail due to local buckling. On the other hand, regarding the tensile rupture, the pipe will fail in operable conditions, but no in pressure integrity. Perhaps these result could be considered as a useful check for design purposes. However, deterministic analysis is of unknown safety. It can be overly conservative or overly unsafe depending on the scenario selected as a baseline. Consistent safety factors cannot be generated for such a single scenario without a full probabilistic analysis. The latter, when done correctly, offers the desired compromise between cost and reliability.

CONCLUSIONS

A methodology for performance assessment of buried pipelines at fault crossing is presented. The seismic hazard analysis is performed at first through an indirect method to quantify the probabilistic nature of fault movement by implementing the Probabilistic Fault Displacement Hazard Analysis (PFDHA). The PFDHA implementation for pipeline – fault crossing accounts for all pertinent seismological parameters and includes the probability of the fault rupture intercepting the pipeline. Epistemic uncertainties are handled through a typical logic tree formulation. The fault displacement is then decomposed to the corresponding components in the three-dimensional space. The two independent such components are selected to form the vector intensity measure to consider the impact of different spatial components of displacement on the pipeline mechanical behavior. The fault offset decomposition is a dominant aspect of the process as it allows the engineer to incorporate a wide range of spatial fault movement values in the seismic hazard analysis, which is crucial to assessing the pipeline behavior due to faulting in light of the uncertain fault movement. A simple and approximate procedure is also introduced to model the principal fault displacement component with respect to the fault type being strike-slip, normal or reverse. Pipeline structural analysis is then performed to account for the effect of fault displacement components on the pipeline and estimate the model demand in terms of maximum developing tensile and compressive strains. Finally, the convolution of seismic hazard and structural response yields the joint hazard surfaces of tensile and compressive strains. Strain hazard surfaces provide all the necessary information regarding the potential of failure due to local buckling or tensile rupture. Furthermore, expressions are presented for estimating the corresponding rates of exceeding specified limit states, considering accordingly demand and capacity uncertainty. The proposed performance assessment process can be an efficient engineering decision making tool with low computational effort and a decisive step towards pipeline performance based design.

ACKNOLEDGMENTS

This research has been co-financed by Greece and the European Social Funds through the Operational Program "Human Resources Development" of the National Strategic Framework (NSRF) 2007-2013 – Project: "Direct Methodology for Performance Based Seismic Design".

REFERENCES

Abrahamson, N. A., and Bommer, J. J., 2005. Probability and uncertainty is seismic hazard analysis, *Earthquake Spectra* **21**(2), 603–607.

ADINA R & D Inc., 2008. *Theory and modeling guide Volume I*: *ADINA*, *Report ARD 08-7*, Watertown, M.A.

American Lifelines Alliance (ALA), 2001. *Guidelines for the Design of Buried Steel Pipe – July 2001* (*with addenda through February 2005*), Washington, D.C.

American Society of Mechanical Engineers (ASME), 2012. *ASME B31-08 – 2012 – Gas transmission and distribution piping systems*, New York, USA.

Angell, M. M., Hanson, K., Swan, H.H., Youngs, R., and Abramson, H., 2003. Probabilistic fault displacement hazard assessment for flowlines and export pipelines, Mad Dog and Atlantis field developments, Deepwater Gulf of Mexico, in *Proceedings*, *2003 Offshore Technology Conference*, 5–8 May, 2003, Houston, USA.

Bazzuro, P., and Cornell, C. A., 2002. Vector-valued probabilistic seismic hazard analysis (VPSHA), in *Proceedings*, *7th U.S. National Conference on Earthquake Engineering*, 21–25 July, 2002, Boston, M.A., U.S.A.

Bommer, J. J., and Scherbaum, G., 2008. The use and misuse of logic trees in probabilistic seismic hazard analysis, *Earthquake Spectra* **24**(4), 997–1009.

Chen, R., and Petersen, M. D., 2011. Probabilistic fault displacement hazards for the Southern San Andreas Fault using scenarios and empirical slips, *Earthquake Spectra* **27**(2), 293–313.

Cornell, C. A., 1968. Engineering seismic risk analysis, *Bulletin of the Seismological Society of America* **58**, 1583–1606.

Cornell, C. A., and Krawinkler, H., 2000. Progress and challenges in seismic performance assessment, *PEER Center News* **3**(2), 1–4.

Gresnigt, A. M., and Karamanos, S. A., 2009. Local buckling strength and deformation capacity of pipes, in *Proceedings of the Nineteenth (2009) International Offshore and Polar Engineering Conference*, 21–26 June, 2009, Osaka, Japan.

Gutenberg, R., and Richter, C. F., 1944. Frequency of earthquakes in California, *Bulletin of the Seismological Society of America* **34**, 185–188.

Karamitros, D. K., Bouckovalas, G. D., Kouretzis, G. D,, and Gkesouli, V., 2011. An analytical method for strength verification of buried steel pipelines at normal fault crossings. *Soil Dynamics and Earthquake Engineering* **31**, 1452-1464.

Liu, A. W., He, Q. M., and Jia, X. H., 2013. Fault displacement hazard analysis for the seismic design of oil and gas pipeline, in *Proceedings*, *Sixth China–Japan–US Trilateral Symposium on Lifeline Earthquake Engineering*, 28 May–1 June, 2013, Chengdu, China.

Moss, R. E., and Ross, Z. E., 2011. Probabilistic fault displacement hazard analysis for reverse faults, *Bulletin of the Seismological Society of America* **101**(4), 1542–1553.

O' Rourke, M. J., and Liu, X., 1999. *Response of Buried Pipelines Subjected to Earthquake Effects*, Multidisciplinary Center for Earthquake Engineering Research, Buffalo, New York.

Vamvatsikos, D., and Cornell, C. A., 2002. Incremental Dynamic Analysis, *Earthquake Engineering and Structural Dynamics* **31**(3), 491-514.

Vazouras, P., Dakoulas, P., and Karamanos, S. A., 2015. Pipe-soil interaction and pipeline performance under strike-slip fault movements. *Soil Dynamics and Earthquake Engineering* **72**, 48-65.

Wells, D. L., and Coppersmith, K. J., 1994. New empirical relationships among magnitude, rupture length, rupture width, rupture area, and surface displacement, *Bulletin of the Seismological Society of America* **84**(4), 974-1002.

Wells, D. L., and Kulkarni, V. S., 2014. Probabilistic fault displacement hazard analysis – sensitivity analyses and recommended practices for developing design fault displacements, in *Proceedings, 10th National Conference in Earthquake Engineering*, *EERI*, 21–25 July, 2014, Anchorage, USA.

Wijewickreme, D., Honegger, D., Mitchell, A., and Fitzell, T. 2005. Seismic vulnerability assessment and retrofit of a major natural gas pipeline system: a case history, *Earthquake Spectra* **21**(2), 539-567.

Wijewickreme, D., Karimian, H., and Honegger, D. 2009. Response of buried steel pipelines subjected to relative axial soil movement. *Canadian Geotechnical Journal* **46**(7), 735-752.

Youngs, R. R. et al., 2003. A Methodology for probabilistic fault displacements hazard analysis (PFDHA), *Earthquake Spectra* **19**(1), 191–219.